HHS Public Access

Author manuscript

Org Biomol Chem. Author manuscript; available in PMC 2018 July 21.

Published in final edited form as:

Org Biomol Chem. 2017 July 21; 15(27): 5689–5692. doi:10.1039/c7ob01074e.

Enzymatic self-assembly of an immunoreceptor tyrosine-based inhibitory motif (ITIM)

Natsuko Nina Yamagata, **Xiaoyi Chen**, **Jie Zhou**, **Jie Li**, **Xuewen Du**, and **Bing Xu**

Department of Chemistry, Brandeis University, 415 South Street, Waltham, Massachusetts 02454, USA

Abstract

Here we show the first example of an immunoreceptor tyrosine-based inhibitory motif (ITIM), LYYYYL, as well as its enantiomeric or retro-inverso peptide, to self-assemble in water via enzyme-instructed self-assembly. Upon enzymatic dephosphorylation, the phosphohexapeptides become hexapeptides, which self-assembly in water to result in supramolecular hydrogels. This work illustrates a new approach to design bioinspired soft materials from a less explored, but important pool of immunomodulatory peptides.

This communication reports enzymatic formation of supramolecular hydrogels of hexapeptides based on immunoreceptor tyrosine-based inhibitory motif (ITIM). Supramolecular hydrogels made of peptides have attracted considerable research interests, particularly, in the biomedical field due to their versatility and applications, such as a scaffold mimicking the native microenvironment necessary for cell–cell and cell–matrix interactions,[1–3] the medium for controlled drug release,[4–6] the promoters for nerve regeneration,[7] the adjuvants for immune stimulation,[8, 9] the motif for developing novel anticancer agents,[10] and the model system for understanding the origin of life.[11] These developments indicate that it is beneficial and necessary for exploring the self-assembly of functional peptides for biomedical applications. Based on this notion, we decided to explore the self-assembly of a special and important type of functional peptides, ITIM, which are present in B-cells, T-cells, and natural killer (NK) cells and play a critical role in the inhibitory signalling process of immune response.[12–16]

We chose to study the self-assembly of ITIM because of its unique role in immune response —when the ITIM is phosphorylated, it has an inhibitory effect; however, when the ITIM is dephosphorylated, it triggers signal activation.[12] Our long-term goal is to develop the assemblies of ITIMs as potential immunomodulation materials in the form of hydrogels,[17–20] but currently, there is little knowledge on the self-assembling behaviour of ITIMs. Based on the previous reports on generating supramolecular hydrogels via dephosphorylation of phosphopeptides[21] and on tyrosine being a naturally-occurring amino acid in the human body,[22] we decided to evaluate the ability of self-assembly and

Correspondence to: Bing Xu.

†Electronic Supplementary Information (ESI) available: [details of any supplementary information available should be included here]. See DOI: 10.1039/x0xx00000x

hydrogelation of ITIMs upon enzymatic dephosphorylation. Based on the well-established consensus sequence of ITIM (where X denotes any amino acid): (Ile/Val/Leu/Ser)-X-Tyr-X-X-(Leu/Val), we chose a sequence of LYY_pYYL (**L-1P**), a peptide consisting of leucine and tyrosine which, when dephosphorylated, becomes a symmetric hexapeptide (**L-1**). Such a symmetry allows the design of its retro-inverso peptide (**RI-1**) to be the same as its enantiomeric peptide (**D-1**), though the relevant phosphopeptides, **D-1P** and **RI-1P**, differ. Our studies reveal that, although these peptides form stable hydrogels likely consisting of beta-sheets, the precursors differ considerably in cytotoxicity (i.e., **L-1P** exhibits higher cytotoxicity than **D-1P** and **RI-1P** do). Among **D-1P** and **RI-1P**, **RI-1P** is more cell compatible. Alkaline phosphatase (ALP) is a ubiquitous membrane protein that catalyzes the hydrolysis of phosphate monoesters and exhibits a variety of functions (e.g., bone mineralization, intestine absorption, early embryogenesis). These important physiological functions then require excellent tolerance to different substrates.[23] As the first case of exploring ITIMs for self-assembly and given that ITIMs are endogenous functional peptides in mammals, this work may ultimately provide a new way to modulate immune responses by combining ITIMs and enzyme-instructed self-assembly (EISA).[24] Although there are many examples of EISA of peptide derivatives, this work is novel because it apply EISA to a bona fide small peptide and its retro-inverso isomer.

As shown in Scheme, among the five hexapeptides of interest, **L-1P** and **D-1P**, and their dephosphorylated forms, **L-1** and **D-1**, are enantiomers. **D-1P** and **RI-1P** are diastereomers, but once dephosphorylated, they produce the same D-enantiomeric hexapeptides (i.e., **RI-1** and **D-1** are ^{D}Leu-(^{D}Tyr)$_4$-^{D}Leu). We prepared the five hexapeptides by standard solid phase peptide synthesis (SPPS)[25, 26] in fair yields (ESI). The crude compounds were purified by reversed-phase high performance liquid chromatography (HPLC) with an overall purified yield at about 60% and reasonable scales (0.1–0.5 g).

As shown in Figure 1, transmission electron microscopy (TEM) reveals that, after the addition of alkaline phosphatase (ALP) to the solutions of the precursors, **L-1**, generated by dephosphorylation of **L-1P**, self-assembles to form long and straight nanofibers with diameters of 8±1 nm, and **D-1**, generated from **D-1P**, forms nanofibers (diameters of 12±2 nm) plus short fibrillar aggregates. However, **D-1**, generated from **RI-1P**, produces largely non-fibrillar aggregates. These results not only indicate that the EISA of **L-1** results in better assembly than the EISA of **D-1** does, but also that the pathway for generating **D-1** determines the morphologies of its assemblies. As expected, upon the addition the ALP, the conversion of **L-1P**, **D-1P**, or **RI-1P** to **L-1**, **D-1**, or **RI-1**, respectively, results in a hydrogel (Fig. 1B). Rheological analysis of the hydrogels formed by enzymatic dephosphorylation of the three phosphopeptides (0.5 wt%) confirms that all hydrogels are viscoelastic (Fig. 1C). The strain sweeps show that the critical strains are at 2%, 5%, or 4% for the hydrogel formed by EISA from **L-1P**, **D-1P**, or **RI-1P**, respectively. The frequency sweeps show that the storage modulus (G') becomes larger than the loss modulus (G") immediately after addition of ALP (into the solution of **L-1P**, **D-1P**, or **RI-1P**), indicating that the hydrogel of **L-1**, **D-1**, or **RI-1** forms after mixing, preceding the frequency sweep analysis. Upon the same addition of ALP to the precursors, the rheological properties of the hydrogel of **D-1** differ from those of **L-1** and **RI-1**. For example, as is evident from the strain sweep analysis,

the storage modulus (G') intersects the loss modulus (G") at 100% for the hydrogels of **L-1** and **RI-1**, while at 50% for the hydrogel of **D-1**. This observation indicates the rate of the dephosphorylation of **D-1P** is slower than those of **L-1P** and **RI-1P**, agreeing with the results of circular dichroism (CD) analysis (*vide infra*).

To determine the secondary structure of the peptides in the hydrogels, we conducted a time-dependent CD analysis of the hydrogels formed by dephosphorylating the phosphopeptides (Fig. 2). The CD spectrum of the hydrogel formed by **L-1** shows a negative peak at 195 nm followed by a positive peak at 210 nm. The hydrogels formed by **D-1** and **RI-1** show the negative band at 210 nm and a positive band at 195 nm, agreeing with the fact that **D-1** (or **RI-1**) is the enantiomer of **L-1**. These results indicate that the molecular assemblies of these hexapeptides adopt well-defined antiparallel β-pleated sheets to form nanofibrils. The time-dependent changes of the CD signals during the formation of these hydrogels indicate that the dephosphorylation of **L-1P** and **RI-1P** and the self-assembly of **L-1** and **RI-1** occur faster than those of **D-1P** and **D-1**. This observation is consistent with the hypothesis that the retro-inverso peptides may have similar properties as the L-peptides.[27]

To determine the role of EISA from the phosphopeptides for its inhibitory activities and biocompatibility, we tested the cell viabilities of three mammalian cell lines (HeLa, Saos-2, and HS-5) treated by the five hexapeptides (ESI). Saos-2 cells have a significantly higher level of ALP expression on the cell surface than most other cancerous cell lines, including HeLa cells. HS-5 cells are bone marrow/stromal cells (fibroblasts) and thus are not cancerous. We chose these three cell lines (i.e., Saos-2, HeLa, and HS-5) to evaluate the relationship between cell compatibility of the phosphohexapeptides and ectoenzyme expression levels on cells.

As shown in Figure 3, all of these molecules are nearly innocuous to HS-5 cells even at a concentration as high as 500 μM. With the exception of **D-1**, the other precursors and hydrogelators exhibit significant cytotoxicities toward Saos-2 cells, with IC_{50} values from 178 – 1196 μM (2^{nd} day). Aside from the fact that **L-1P** inhibits the growth of HeLa cells considerably, the other four peptides are almost innocuous to HeLa cells. An interesting trend observed in the viability assay is the moderate cytotoxicities of **L-1P** and **L-1**, which may be an inherent feature of the ITIM hydrogels.

Figure 4 shows the cell compatibility of the phosphopeptides on HeLa cells at or above the hydrogelation concentration (0.5 wt %) overnight by mimicking the cellular environment with a hydrogel produced by **L-1P**, **D-1p**, or **RI-1P** via EISA. The proliferation of the cells largely follows the results from Figure 3. That is, among the hydrogels produced from the three precursors, the hydrogel formed by EISA from **RI-1P** is the most compatible to HeLa cells. However, we have little understanding of the different mechanisms of cell death due to peptidic stereochemistry, which needs further investigation. MTT assays shown the viability of HeLa exceeds 100% upon the treatment of **D-1**, implying that **D-1** likely enhances the metabolism of HeLa cells.

In conclusion, this work illustrates the first case of EISA of ITIM peptides and investigates their self-assembly and cytotoxicities in different forms. The cytotoxicity of **RI-1P** (or

D-1P) towards Saos-2 cells, but not to HeLa and HS-5 cells, likely originates from the high-level expression of ALPs on the cell surface of Saos-2.[28] There are other possible causes for the difference in cytotoxicity. Although such unanswered questions remain to be addressed, this work establishes the feasibility of forming hydrogels or supramolecular assemblies of ITIM from EISA processes.

Supplementary Material

Refer to Web version on PubMed Central for supplementary material.

Acknowledgments

This work was partially supported by NIH (R01CA142746) and NSF (MRSEC-1420382). NY thanks the Jordan-Dreyer Summer Research Fellowship. JZ is a HHMI international fellow.

References

1. Song Y, Zhang D, Lv Y, Guo X, Lou R, Wang S, Wang X, Yu W, Ma X. Carbohydr Polym. 2016; 153:652–662. [PubMed: 27561537]
2. Tibbitt MW, Anseth KS. Biotechnol Bioeng. 2009; 103:655–663. [PubMed: 19472329]
3. Yuan D, Xu B. J Mater. Chem. B. 2016; 4:5638–5649.
4. Liang G, Yang Z, Zhang R, Li L, Fan Y, Kuang Y, Gao Y, Wang T, Lu WW, Xu B. Langmuir. 2009; 25:8419–8422. [PubMed: 20050040]
5. Zhang Z, He Z, Liang R, Ma Y, Huang W, Jiang R, Shi S, Chen H, Li X. Biomacromolecules. 2016; 17:798–807. [PubMed: 26830342]
6. Wang W, Hui PC, Wat E, Ng FS, Kan CW, Wang X, Wong EC, Hu H, Chan B, Lau CB, Leung PC. Colloids Surf B Biointerfaces. 2016; 148:526–532. [PubMed: 27690241]
7. Silva GA, Czeisler C, Niece KL, Beniash E, Harrington DA, Kessler JA, Stupp SI. Science. 2004; 303:1352. [PubMed: 14739465]
8. Rudra JS, Tian YF, Jung JP, Collier JH. Proceedings of the National Academy of Sciences of the United States of America. 2010; 107:622–627. [PubMed: 20080728]
9. Tian Y, Wang H, Liu Y, Mao L, Chen W, Zhu Z, Liu W, Zheng W, Zhao Y, Kong D, Yang Z, Zhang W, Shao Y, Jiang X. Nano Letters. 2014; 14:1439–1445. [PubMed: 24564254]
10. Feng Z, Wang H, Du X, Shi J, Li J, Xu B. Chem Commun (Camb). 2016; 52:6332–6335. [PubMed: 27087169]
11. Liu P, Ni R, Mehta AK, Childers WS, Lakdawala A, Pingali SV, Thiyagarajan P, Lynn DG. Journal of the American Chemical Society. 2008; 130:16867–16869. [PubMed: 19053426]
12. Janeway, CJ., Travers, P., Walport, M., Shlomchik, MJ. Immunobiology: The Immune System in Health and Disease. 5. Garland Science; New York: 2001.
13. Lanier LL. Nature Immunology. 2001; 2:23–27. [PubMed: 11135574]
14. Lanier LL. Current Opinion in Immunology. 2003; 15:308–314. [PubMed: 12787756]
15. Long EO. Annual Review of Immunology. 1999; 17:875–904.
16. Ravetch JV, Lanier LL. Science. 2000; 290:84–89. [PubMed: 11021804]
17. Grenfell RFQ, Shollenberger LM, Samli EF, Harn DA. Clinical and Vaccine Immunology. 2015; 22:336–343. [PubMed: 25609075]
18. Mammadov R, Cinar G, Gunduz N, Goktas M, Kayhan H, Tohumeken S, Topal AE, Orujalipoor I, Delibasi T, Dana A, Ide S, Tekinay AB, Guler MO. Scientific Reports. 2015; 5:16728. [PubMed: 26577983]
19. Monette A, Ceccaldi C, Assaad E, Lerouge S, Lapointe R. Biomaterials. 2016; 75:237–249. [PubMed: 26513416]

20. Vishwakarma A, Bhise NS, Evangelista MB, Rouwkema J, Dokmeci MR, Ghaemmaghami AM, Vrana NE, Khademhosseini A. Trends in Biotechnology. 2016; 34:470–482. [PubMed: 27138899]
21. Yang ZM, Liang GL, Xu B. Accounts of Chemical Research. 2008; 41:12.
22. Bankovich AJ, Raunser S, Juo ZS, Walz T, Davis MM, Garcia KC. Science. 2007; 316:291. [PubMed: 17431183]
23. Sharma U, Pal D, Prasad R. Indian J. Clin. Biochem. 2014; 29:269–278. [PubMed: 24966474]
24. Yang ZM, Gu HW, Fu DG, Gao P, Lam JK, Xu B. Advanced Materials. 2004; 16:5.
25. Coin I, Beyermann M, Bienert M. Nat. Protocols. 2007; 2:3247–3256. [PubMed: 18079725]
26. Ottinger EA, Shekels LL, Bernlohr DA, Barany G. Biochemistry. 1993; 32:4354–4361. [PubMed: 7682846]
27. Fletcher MD, Campbell MM. Chemical Reviews. 1998; 98:763–796. [PubMed: 11848914]
28. Zhou J, Xu B. Bioconjugate Chemistry. 2015; 26:987–999. [PubMed: 25933032]

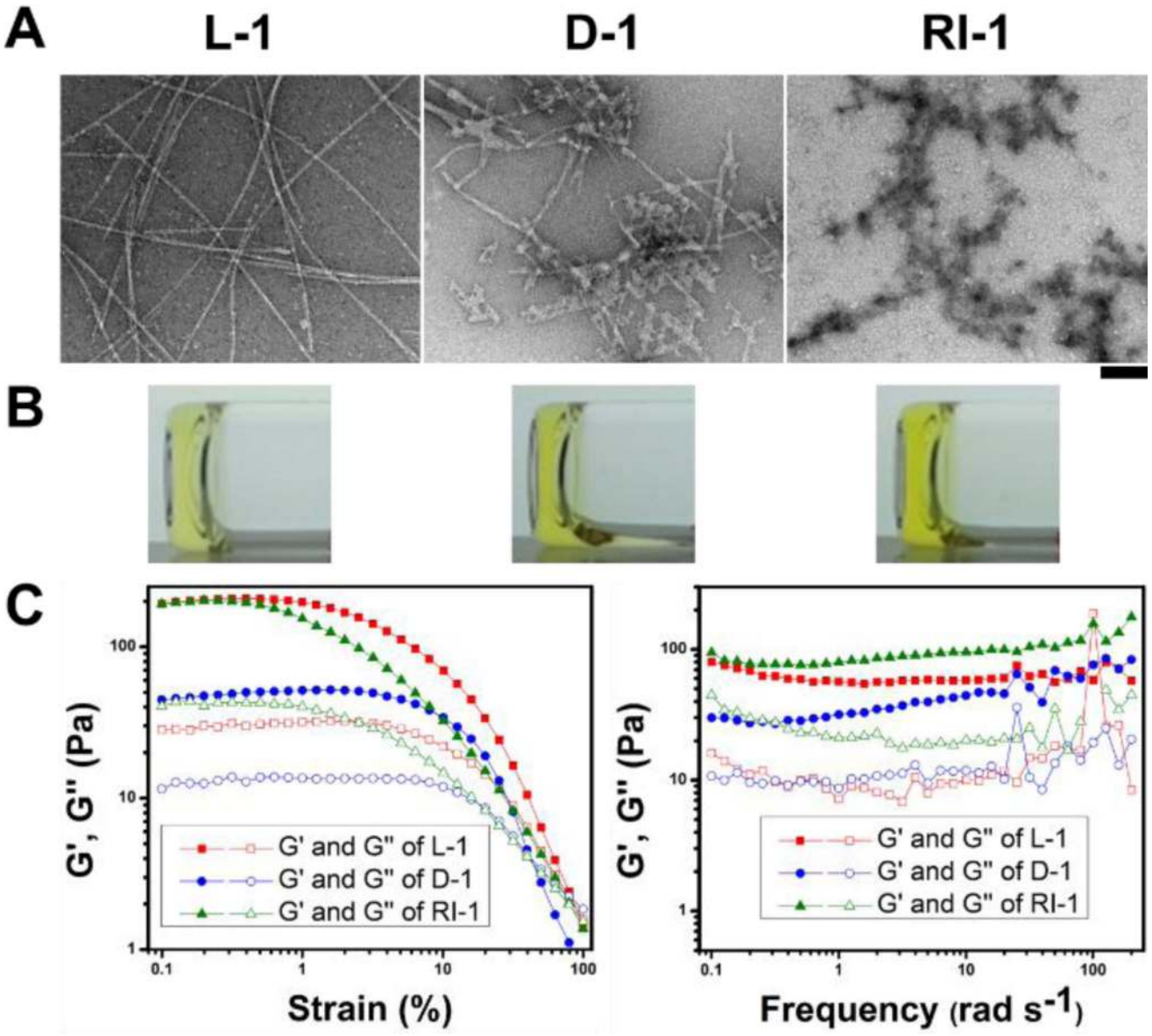

Figure 1.

(A) TEM images of the nanostructures formed overnight by adding ALP (10 U/mL) in the PBS buffered solutions of the phosphopeptides (**L-1P**, **D-1P**, and **RI-1P**; 0.5 wt% at pH 7.4). Scale bar is 100 nm. (B) Optical images of the hydrogels corresponding the TEM above them. (C) Rheological properties of the hydrogels of the hexapeptides: strain sweep (left); frequency sweep (right).

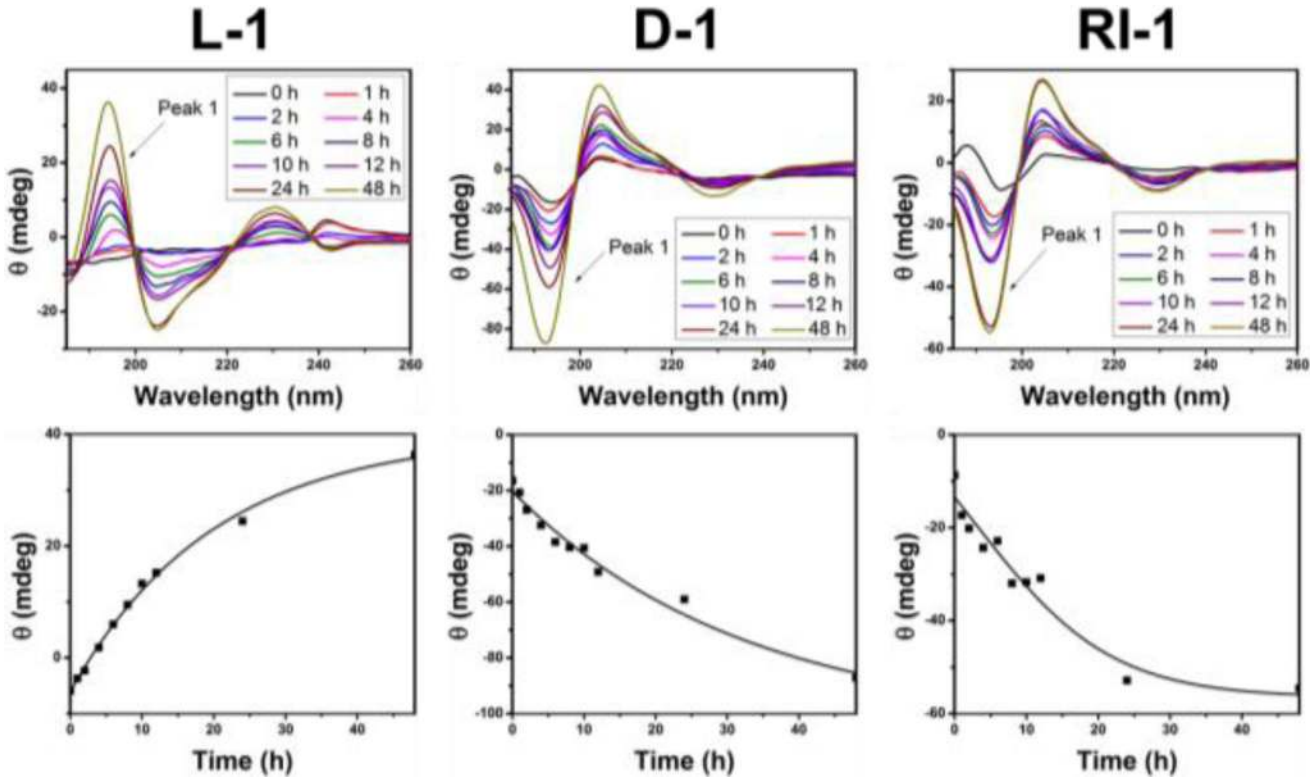

Figure 2.

Time dependent CD analysis (top panel) and time-intensity graphs (bottom panel) of hydrogels, formed upon the addition of ALP (10 U/mL) to solutions of corresponding precursors at concentration of 0.5 wt% and scanned at desired times. The time-intensity graphs for the EISA of **L-1**, **D-1**, and **RI-1** are 0^{th} order (rate = k), with initial apparent rate constants of 1.82, 2.46, and 1.68, respectively.

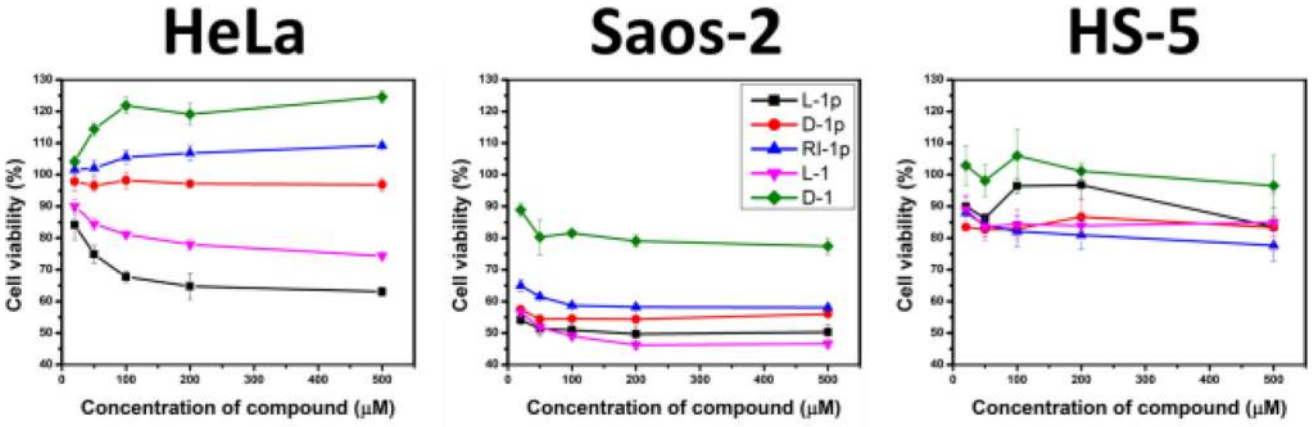

Figure 3.

MTT viability assay summary (2nd day of incubation) of HeLa, Saos-2, and HS-5 cells treated with five hexapeptides at concentrations up to 500 μM. (Full data available in SI; Fig. S6)

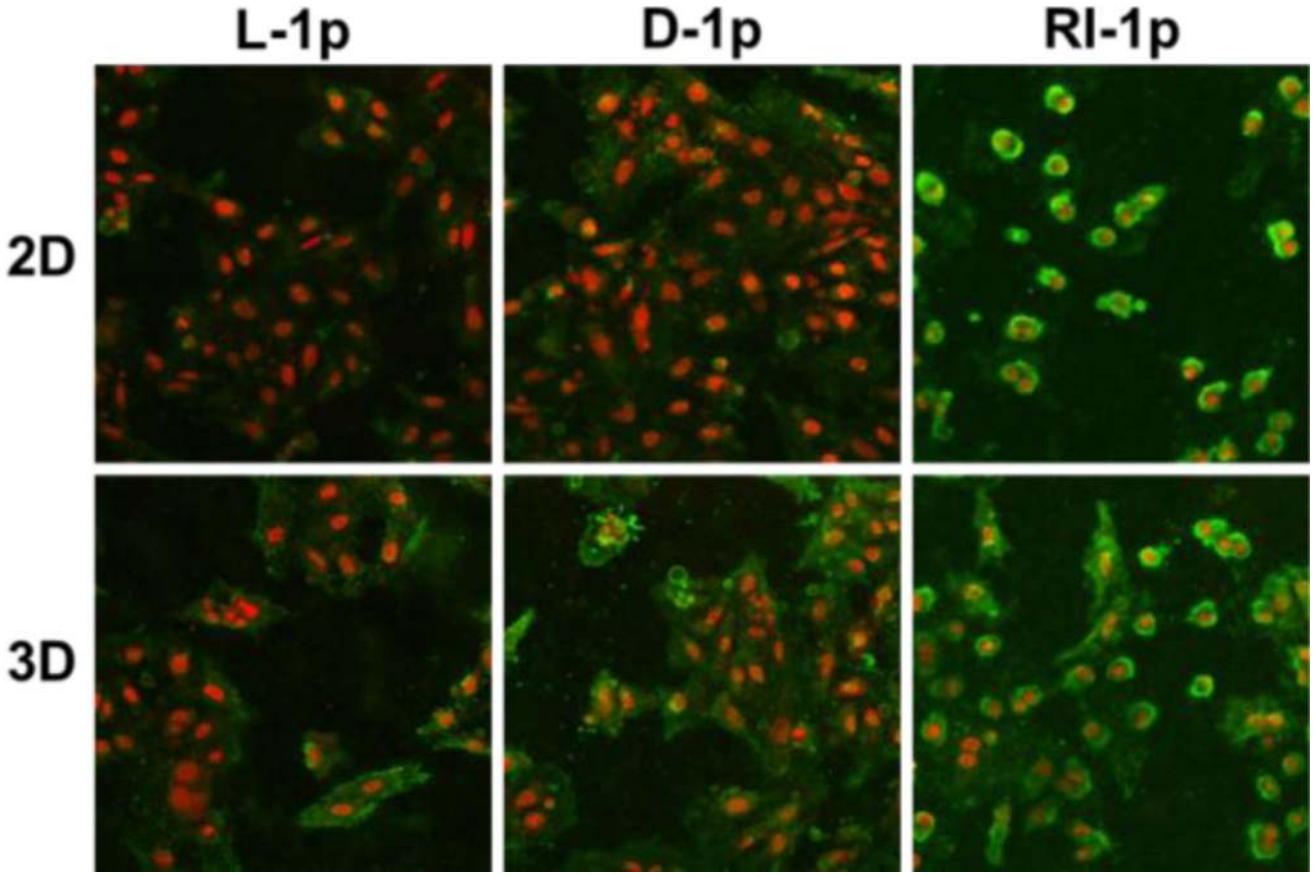

Figure 4.

Fluorescent images of 2D (cells on gel) and 3D (cells in gel) live/dead cell assay of HeLa cells treated for 24h with 300 μL of 0.5 wt.% gels formed by **L-1P**, **D-1P**, and **RI-1P** via EISA for 24 hours.

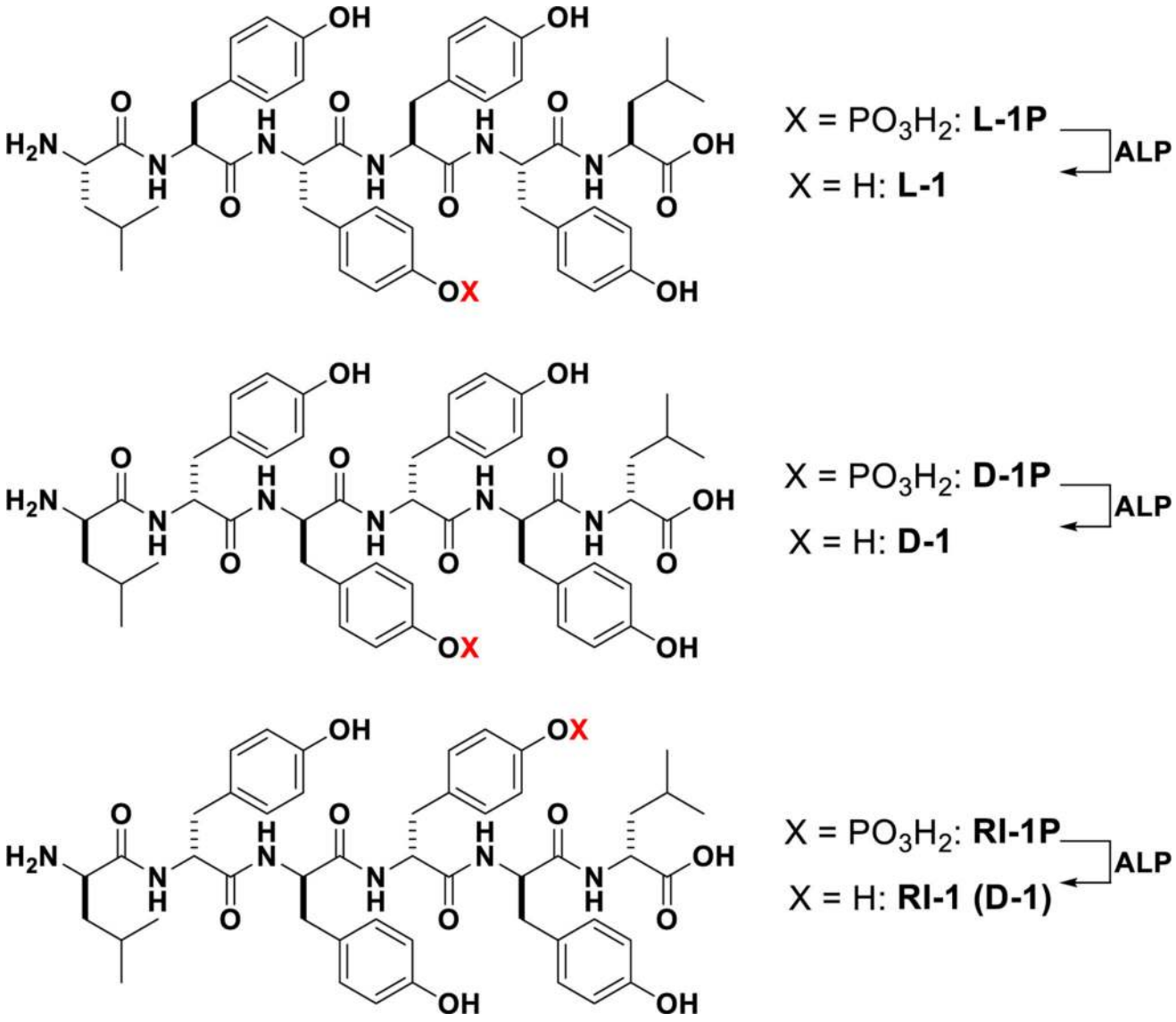

Scheme 1.

ITIM-based molecular structures of the three phosphopeptides and the corresponding dephosphorylated hexapeptides.